



Is the tropical cyclone surge in Shanghai more sensitive to landfall location or intensity change?

Shuai Wang¹  | Ralf Toumi¹ | Qinghua Ye^{2,3} | Qian Ke³ |
Jeremy Bricker^{3,4} | Zhan Tian⁵  | Laixiang Sun^{6,7}

¹Department of Physics, Imperial College London, London, UK

²Deltares, Delft, Netherlands

³Department of Hydraulic Engineering, Faculty of Civil Engineering and Geosciences, Delft University of Technology, Delft, Netherlands

⁴Department of Civil and Environmental Engineering, University of Michigan, Ann Arbor, Michigan

⁵School of Environmental Science and Engineering, Southern University of Science and Technology of China, Shenzhen, China

⁶Department of Geographical Sciences, University of Maryland, College Park, Maryland

⁷School of Finance and Management, SOAS University of London, London, UK

Correspondence

Zhan Tian, School of Environmental Science and Engineering, Southern University of Science and Technology of China, Shenzhen 518055, China.
Email: tianz@sustech.edu.cn

Funding information

Engineering and Physical Sciences Research Council, Grant/Award Number: R034214/1; National Natural Science Foundation of China, Grant/Award Number: 51761135024; Netherlands Organization for Scientific Research, Grant/Award Number: ALWSD.2016.007

Abstract

It has been shown that the proportion of intense tropical cyclones (TCs) has been increasing together with a poleward migration of TC track. However, their relative importance to TC surge at landfall remains unknown. Here we examine the sensitivity of TC surge in Shanghai to landfall location and intensity with a new dynamical modelling framework. We find a surge sensitivity of $0.8 \text{ m } (^{\circ}\text{N})^{-1}$ to landfall location, and $0.1 \text{ m } (\text{m s}^{-1})^{-1}$ to wind speed in Shanghai during landfall. The landfall location and intensity are comparably important to surge variation. However, based on a plausible range of reported trends of TC poleward migration and intensity, the potential surge hazard due to poleward migration is estimated to be about three times larger than that by intensity change. The long-term surge risk in Shanghai is therefore substantially more sensitive to changes of TC track and landfall location than intensity. This may also be true elsewhere and in the future.

KEYWORDS

climate change, landfall, storm surge, tropical cyclone

1 | INTRODUCTION

Tropical cyclone (TC) related hazards pose the greatest threat to coastal regions (Pielke *et al.*, 2008; Rappaport, 2014), especially in East Asia where the population and economy are growing rapidly and are

vulnerable to natural hazards (Small and Nicholls, 2003). China has the highest rate of TC landfalls in the world (Fudeyasu and Wang, 2011), and China's coastal provinces, exposed directly to landfall TC hazards, account for more than half of China's GDP in 2019. Shanghai, the financial centre of China, is ranked as a top-10 city in the

This is an open access article under the terms of the Creative Commons Attribution License, which permits use, distribution and reproduction in any medium, provided the original work is properly cited.

© 2021 The Authors. *Atmospheric Science Letters* published by John Wiley & Sons Ltd on behalf of the Royal Meteorological Society.

world in terms of population and assets exposed to coastal flooding (Hanson *et al.*, 2011). On average there is less than one landfalling TC directly influencing Shanghai per year (Fogarty *et al.*, 2006), and yet it can come at significant cost. Typhoon Winnie (1997), for example, caused a loss of \$91 million to the city due to the concurrence of strong surge and high astronomical tide at landfall (Wang *et al.*, 2018).

Extreme winds and storm tide happen concurrently during TC landfall. The storm tide is a nonlinear combination of astronomical tide and storm surge, which is challenging to assess due to the nonlinear interactions between the atmosphere, ocean and bottom topography (Anthes, 1982). Storm surge depends on ocean depth/shelf width combined with TC characteristics, for example, the landfall location, intensity (Harris, 1963), size (Irish *et al.*, 2008), approaching speed (Rego and Li, 2009) and angle (Weisberg and Zheng, 2006). The dependence of surge on wind more than pressure closer to land is predominantly a function of ocean depth. For open ocean islands with a narrow continental shelf the pressure component can end up being a more important factor of surge (Joyce *et al.*, 2019). For marginal and shelf seas positive surge occurs where winds are blowing onshore (Wong and Toumi, 2016b). In the North Hemisphere, this requests the region of interest locating on the right-hand side of landfall location along the TC track. The magnitude of positive surge is then driven primarily by wind stress and atmospheric pressure gradient (Jelesnianski, 1966; Anthes, 1982), with the dependence on wind much stronger than pressure when moving close to land (Wong and Toumi, 2016a). Therefore, the maximum surge at landfall commonly happens to the right-hand side (in the North Hemisphere) of landfall location close to the radius of maximum surface wind.

The surge induced by landfall TCs may be modulated by the climatic changes of TC intensity and/or geographical distribution of TC tracks. Emanuel (2005) showed that the destructive potential of TCs has been rising since the 1970s due to the increase in the sea surface temperature (SST). The poleward migration of the location of TC lifetime maximum intensity (LMI) (Kossin *et al.*, 2014), probably driven by tropical expansion (Sharmila and Walsh, 2018), may also potentially increase TC-related hazards in the regions at higher latitudes (Kossin *et al.*, 2016). The poleward migration is particularly well observed in the western North Pacific (Knutson *et al.*, 2019). This change may shift TC activity from the South China Sea to the East China Sea (Knutson *et al.*, 2020) and the surge risk at Shanghai may consequently increase.

The prediction and planning for TC surge is crucial for preventing casualties and economic damage. The prediction of TC surge involves statistical and dynamical

approaches. Conner *et al.* (1957) developed an empirical method for maximum surge forecasting with TC intensity as a singular input. The Sea, Lake, and Overland Surges for Hurricanes (SLOSH) model (Jelesnianski, 1992), developed by the National Weather Service back to the 1970s, is a widely used dynamical surge model and remains in operation at the National Hurricane Center. The SLOSH model applies a parametric TC surface wind field constructed with a few readily obtained TC characteristics, which is a compromise between the operational efficiency and the accuracy of TC wind field. Bruyère *et al.* (2019) emphasised the importance of dynamical representation of TC landfall scenarios to risk assessment and developed a hybrid cyclone model with idealised atmospheric configuration and realistic topography and coastlines. However, their hybrid model was not coupled with a hydrodynamical component to simulate TC surge which we are doing here for the first time for Shanghai. With such an integration of full-physics atmospheric and hydrodynamic models the TC surface wind field can evolve more realistically during landfall, and therefore the storm surge in Shanghai can be simulated more accurately in difference TC landfall scenarios.

The objective of this study is to (i) develop a dynamical modelling framework for TC surge with a flexible-mesh hydrodynamical model forced by a full-physics atmospheric model, and (ii) evaluate the relative importance of TC landfall location and intensity to surge in Shanghai. The following section will introduce the model setup and experiment design. Section 3 will show the results of the simulated surge and surge sensitivity to landfall location and intensity. The last two sections will discuss the results and summarise the study.

2 | METHODS

2.1 | Atmospheric model setup

The TC simulation is conducted with the Weather Research and Forecasting (WRF) Model (Skamarock *et al.*, 2008, version 4.1). Three square nested domains (800×800 grids), each with 41 σ levels in the vertical, are implemented with a horizontal grid spacing of 12, 4 and 1.33 km, respectively, on an f plane (20°N) with horizontally uniform SST. Three domains are two-way interactive with the inner two domains following the TC centre. Full-physics parameterisation is used as in Wang and Toumi (2019) to account for radiation, microphysics, planetary boundary layer and surface layer processes. Considering that the innermost domain with 1.33-km grid resolution (about $1,000 \times 1,000$ km) is large enough to cover the main convection region in a TC, the cumulus scheme is not applied in any domain.

The TC simulation is initiated on an idealised aquaplanet in a stationary environment. The initial bogus vortex is specified from an analytic wind profile model (Wang and Toumi, 2016). The initial atmospheric sounding profiles for different SSTs are adopted from Wang and Toumi (2018b). Note that the initial soundings are adjusted to the underlying SST to reach the radiative-convection equilibrium before any storm simulation. The model is integrated for 5 days to have the TC fully developed, that is, the intensity reaches the LMI. In the second stage of simulation, we restart the simulation and add in a vertically uniform steering flow to convey the TC towards the Northwest. The background steering flow is added via the boundary condition and fixed at 4 m s^{-1} (2.83 m s^{-1} of easterly and poleward winds) at the lateral boundary throughout the landfall simulation. Nudging technique is not applied and there is no horizontal relaxation distance specified. At the start of the second stage of simulation, we also add in the topography and coastlines within the radius of 1,000 km around Shanghai to the northwest of the TC. At the beginning of the restart run, Shanghai is about 1700 km away from the TC centre. The simulated TCs make landfall around Shanghai in the fifth simulation day of the second-stage simulation. The second-stage simulation lasts for 7 days so that a complete intensity decay after landfall can be properly simulated.

2.2 | Hydrodynamical model setup

Once a WRF simulation is completed, the model surface wind, pressure and rainfall are used to force the Delft3D D-Flow Flexible Mesh hydrodynamical model. It is a newly developed shallow water solver using unstructured grid (De Goede, 2020). The governing equations include continuity equation and momentum equations (Kernkamp *et al.*, 2011). The finite volume numerical scheme is applied to compute hydrodynamics, and substance transport in river, estuary and coastal waters (Kernkamp *et al.*, 2011; Martyr-Koller *et al.*, 2017). The model has been calibrated and validated with observed surge and tidal levels at 10 stations around Shanghai during Typhoon Winnie in 1997 (Ke *et al.*, 2021). Surge level is calculated as the difference between total water levels with and without forcings by a TC in the hydrodynamical model.

2.3 | Experiment design

A suite of experiments is conducted by varying the SST and landfall location around Shanghai (Table S1). The purpose of the SST experiments is to vary the TC

intensity at landfall in a physically plausible way so that a linear sensitivity of surge to landfall intensity can be derived. In this sense the SST in the control experiment (CTRL_0), set as 27.0°C , does not have to accurately reflect the mean climatological SST around Shanghai. Based on CTRL_0 five more simulations are conducted to simulate TCs making landfall to the north and south of Shanghai by only tuning the background steering flow. These six simulations are then reproduced by increasing the SST by 1°C and 2°C , respectively. This approach generates 18 cases.

2.4 | Observations

The TC best track data are from the China Meteorological Administration. The maximum surface wind speed and latitude of TC landfall are calculated along China's coastline (31.2°N to 27.0°N) for the period 1949–2018. The Wusong tide gauge station is located at the estuary of the Huangpu River. Any extreme surge reaching this station may severely raise the water level in the upstream of the river and then potentially lead to dike breach and flooding in the downtown region (Figure S1).

3 | RESULTS

The tracks of CTRL_0, SST1_0 and SST2_0 pass through Shanghai with Wusong station to the right-hand side of the TC eyewall where the onshore wind is expected to be the strongest (Figure 1a). Wusong station is exposed to easterly (onshore) wind in 12 simulations with the landfall location to the south of the station, and westerly (offshore) wind in the other 6 simulations in which the landfall is to the north.

The all cases mean TC intensity—measured by the maximum surface wind speed—stabilises above 50 m s^{-1} as a category-3 TC for simulation hour 24–96 (Figure 1b). During this period, the mean intensity is 51 m s^{-1} for the experiments with an SST at 27°C , 53 m s^{-1} at 28°C and 57 m s^{-1} at 29°C , respectively. This gives a sensitivity of about 6% of intensity increase per degree SST increase. TC intensity decays rapidly post landfall after hour 96 with a mean rate of 15 m s^{-1} per day. With the dynamical atmospheric model the complexity of TC intensity evolution can be physically simulated during landfall.

Figure 2a shows that the maximum surge is to the right of the track where the wind is stronger due to the combination of swirling and transition. This asymmetric surge pattern is clearer when a TC approaches land. A

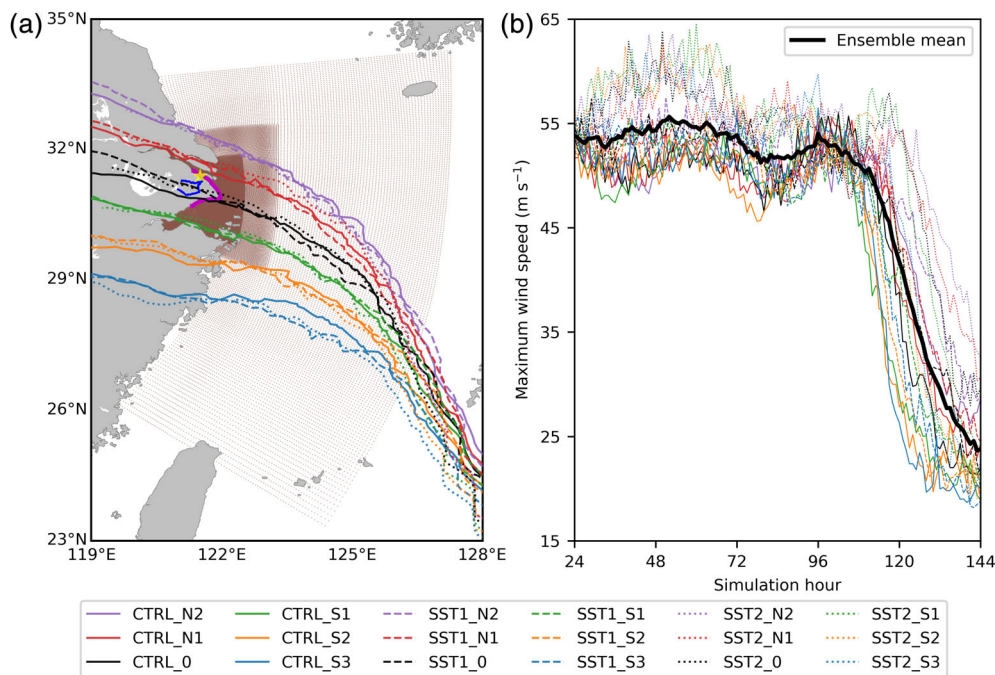


FIGURE 1 Simulated TC (a) tracks and (b) intensity time series. The simulation hour in (b) shows the simulation time in the second stage of simulation. Shanghai shoreline (magenta line). Huangpu River (dark solid blue line). Wusong station (yellow star). Hydrodynamical model grid mesh (brown dots)

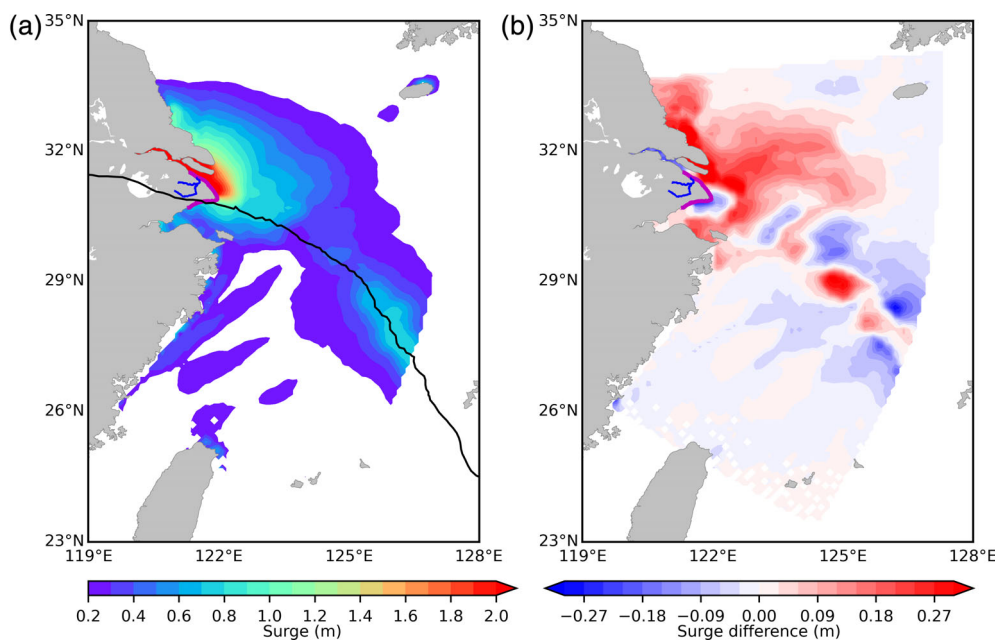


FIGURE 2 Surge footprint of (a) simulation CTRL_0 and (b) the differences between SST1_0 and CTRL_0. The black line in (a) shows the simulated TC track in CTRL_0. Shanghai shoreline (magenta line). Huangpu River (dark solid blue line)

more intense TC under higher SST leads to a higher surge as expected (Figure 2b).

When landfall location moves from the south to north towards Shanghai (31.2°N), the maximum wind during landfall increases at Wusong station, and consequently, the local surge rises (Figure 3). For the same landfall location, Figure 3 also shows a slight reduction of surge height for the same local wind speed when the SST increment changes from $+1$ to $+2^{\circ}\text{C}$. This may be due to a smaller TC size with higher SST (Figure S2), which is consistent with recent observations (Lavender and

McBride, 2020). The important point is that these size effects are much smaller than the range of wind speeds we examine here. When the landfall location shifts to the north of Shanghai, the maximum surface wind at Wusong station remains around the hurricane-force level (33 m s^{-1}), but the local surge height is reduced to less than 1 m (not shown in Figure 3). This is because of the change in offshore wind direction at Wusong station when Shanghai is located on the left of the track. The relationships in Figure 3 are significant ($p \leq .05$) between surge and wind speed/landfall location. The surge

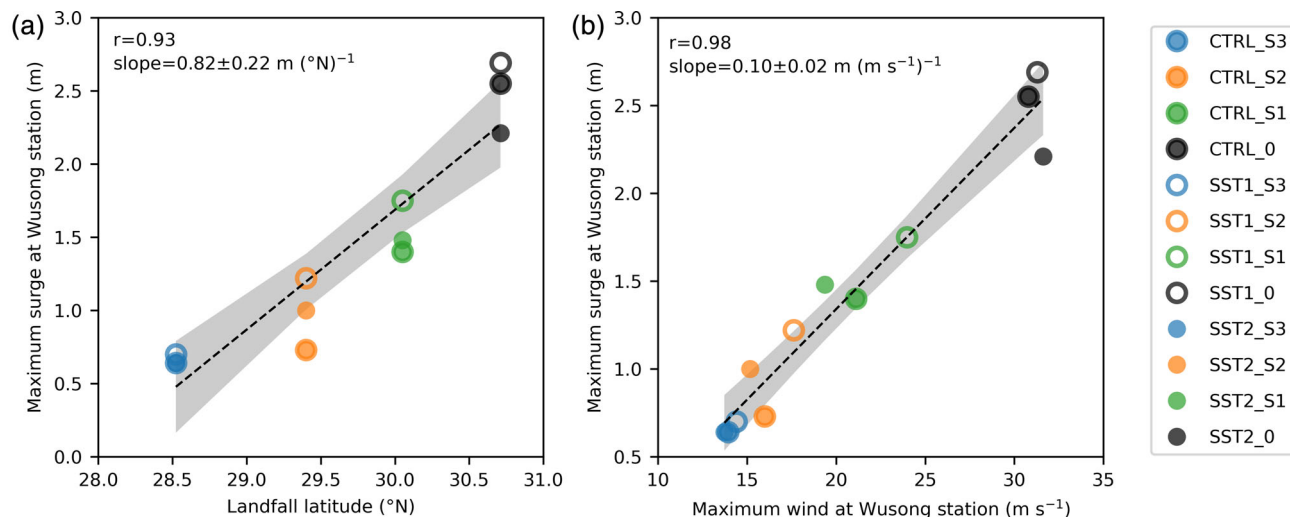


FIGURE 3 Maximum TC surge at Wusong station and (a) TC landfall location and (b) maximum wind at Wusong station during landfall. The TC landfall locations are all to the south of Wusong station. The dashed lines show the linear fit (least squares regression) with 95% confidence intervals denoted by the shading. The Pearson correlation coefficient (r) and linear slope ($\pm 95\%$ confidence intervals) are given in the top-left corner in (a) and (b)

sensitivities are $0.82 \pm 0.22 \text{ m } (^\circ\text{N})^{-1}$ to landfall location, and $0.10 \pm 0.02 \text{ m } (\text{m s}^{-1})^{-1}$ to maximum local wind.

To convert these sensitivities to potential changes of surge hazard over recent decades, we need to know the historical trends of intensity and landfall location. The reported trends depend on the data and analysis procedure. Rather than fix on one trend estimate here we will use a range of plausible values. This is sufficient to allow us to compare the different potential contributions of intensity and landfall location to surge variation. Park *et al.* (2014) showed a range of annual trend in TC landfall intensity of $0.6\text{--}1.8 \text{ m s}^{-1}$ per decade in East Asia. The reported range of poleward migration of TC lifetime maximum intensity is $0.4\text{--}1.0^\circ\text{N}$ per decade (Kossin *et al.*, 2014, 2016; Sun *et al.*, 2019). Combining these observed trends with the surge sensitivity in our simulations, we find a potential surge trend of $0.1\text{--}0.2 \text{ m}$ per decade due to TC intensity change, but a much larger $0.3\text{--}0.8 \text{ m}$ per decade due to poleward migration of TC locations. If we take the central value as the best estimate, landfall location change is at least three times more important than wind speed change. Therefore, the long-term change in potential surge hazard in Shanghai is much more sensitive to the change in TC track than intensity.

4 | DISCUSSION

The atmospheric configuration of our hybrid TC-surge model is similar to Bruyère *et al.* (2019). Such a semi-idealised setup with real topography is a useful tool of

exploring the worst-case scenario of hazard impact induced by landfalling TCs. Our improvement here is to integrate this atmospheric modelling setup with a state-of-the-art hydrodynamical model for surge investigation. Previous studies have combined WRF with other hydrodynamical models (e.g., Mori *et al.*, 2014), but they are all designed for real TC case studies and therefore constrained by specific environmental conditions during the TC passage. Our new hybrid TC-surge modelling framework can produce realistic physical scenarios for wind and surge during a TC landfall, which can be used to explore worst-case scenarios for the location of interest.

We find the surge sensitivity to intensity of $0.10 \pm 0.02 \text{ m } (\text{m s}^{-1})^{-1}$. A similar sensitivity can be obtained with the Saffir-Simpson Hurricane Scale warning system (Simpson and Saffir, 1974), which estimates the surge height for five TC intensity categories. By linearly interpolating surge level with 1 m s^{-1} intervals of all the categories, we obtain a surge sensitivity of $0.13 \pm 0.01 \text{ m } (\text{m s}^{-1})^{-1}$. Wong and Toumi (2016b) showed that a TC with a maximum wind speed of 77 m s^{-1} can generate a surge of 5.4 m at landfall in an idealised modelling framework. This implies a linear surge sensitivity to wind intensity of about $0.07 \text{ m } (\text{m s}^{-1})^{-1}$, which is also close to the sensitivity in our simulations. The possibility of size changes under warming (Xu and Wang, 2010; Sun *et al.*, 2017; Wang and Toumi, 2018b; Bruneau *et al.*, 2020) also does not change the sensitivity markedly. The local wind speed is the dominant source of surge height-wind sensitivity. It is noteworthy that the discussion here does not consider the surge dependence on ocean depth and continental shelf width. The consistency between our

results and previous studies suggests general applicability of our surge-to-wind sensitivity.

We also find the surge sensitivity to landfall location of $0.82 \pm 0.22 \text{ m } (^{\circ}\text{N})^{-1}$. This can be understood in term of the radial TC wind profile. Chan and Chan (2015) and Wang and Toumi (2018a) find a global mean wind radii of gale-force wind (18 m s^{-1}) and damaging-force wind (26 m s^{-1}) of about 200 and 100 km, respectively. This change implies the surface wind at the location of interest may be increased by about 8 m s^{-1} (from gale-force to damaging-force) due to a poleward migration of TC landfall by 1° latitude towards this location from the South, that is, $8 \text{ m s}^{-1} (^{\circ}\text{N})^{-1}$. This sensitivity is confirmed by our analysis (Figure 3). Combining the surge sensitivity to wind of $0.1 \text{ m } (\text{m s}^{-1})^{-1}$, we obtain a surge sensitivity to poleward migration of TC landfall of 0.8 m per degree latitude change, which agrees well with our simulations. Two inferences may then be made. Firstly, our simulated surge sensitivity to landfall location and intensity can be applied in Shanghai, but may also be true elsewhere. Secondly, the important role of landfall location is due in part to the radial reduction of wind outwards from TC centre.

We now consider case-by-case variations. The standard deviation of landfall latitude and intensity in our Shanghai region (Section 2.4) is 1°N and 11 m s^{-1} , respectively, and they are independent ($r = -0.16$, $p = .37$). By multiplying the sensitivities [$0.8 \text{ m } (^{\circ}\text{N})^{-1}$ for location and $0.1 \text{ m } (\text{m s}^{-1})^{-1}$ for intensity] by the variations, the surge variability is estimated to be 0.8 m and 1.1 m due to landfall location and intensity variations, respectively. Thus, the landfall intensity is as important as the landfall location to case-by-case surge variability. However, for long-term change in potential surge hazard, our results have shown that the historical poleward migration of TC locations is at least three times more important to surge than the increase of TC intensity.

Our simulation shows a relatively weak dependence of TC maximum intensity on SST change. This is consistent with previous studies showing that the sensitivity of TC maximum intensity to SST is only about 3–4% $^{\circ}\text{C}^{-1}$ under the radiative-convective equilibrium (Knutson and Tuleya, 2004; Knutson *et al.*, 2015; Yoshida *et al.*, 2017; Wang and Toumi, 2018b). The global mean SST has increased by half a degree in the past half-century and perhaps another 1° by 2050. Under equilibrium assumption this would lead to only 3–4% of increase in TC maximum wind speed (about 2 m s^{-1} increase for a category-3 TC). This change in intensity would yield a small change in surge (only about 0.2 m). On the other hand, Kossin *et al.* (2014) showed that the poleward migration in the

western North Pacific has been about 0.3°N per decade. If we assume the landfall location shares the same trend from 27°N to the latitude of Shanghai and continues in the future, the poleward migration of landfall location to 2050 would be about 1° latitude northward. This latitudinal shift of TC tracks may lead to a dramatic potential change of surge by 0.8 m, about four times larger than the change induced by the intensity increase of a category-3 TC. This suggests the possible future relative importance of poleward migration of TC location to surge hazard in Shanghai.

The main uncertainties in this study arise due to uncertain trends of TC poleward migration. This is why we focus on a range of values. We assume the whole TC track shifts to higher latitudes. However, a robust and significant poleward migration of TC lifetime maximum intensity and genesis location has been only confirmed in the western North Pacific (Kossin *et al.*, 2014; Daloz and Camargo, 2018). Murakami *et al.* (2020) showed a clear poleward shift of TC frequency along the east China coast for 1980–2018. Liu and Chan (2019) found that the mean landfall intensity is increasing at the east coast of China due to more frequent landfalls by intense typhoons.

5 | CONCLUSIONS

In this study, we develop a new dynamical modelling framework for TC surge with a full-physics atmospheric model forcing a hydrodynamical model. We find a surge sensitivity of $0.8 \text{ m } (^{\circ}\text{N})^{-1}$ to TC landfall location, and $0.1 \text{ m } (\text{m s}^{-1})^{-1}$ to wind speed in Shanghai during landfall. Considering the case-by-case variation of TC surge, the landfall location and intensity contribute comparably to the variation of surge in Shanghai. However, based on a plausible range of reported past trends the long-term surge level in Shanghai is at least three times more sensitive to changes of TC landfall location than intensity. The landfall location change therefore likely plays a dominant role in the future climatic change of TC surge risk in Shanghai, and this may also be true elsewhere.

AUTHOR CONTRIBUTIONS

Shuai Wang: Conceptualization; formal analysis; methodology; writing-original draft; writing-review & editing. **Ralf Toumi:** Conceptualization; funding acquisition; writing-review & editing. **Qinghua Ye:** Formal analysis; methodology; writing-review & editing. **Qian Ke:** Writing-review & editing. **Jeremy Bricker:** Funding acquisition; writing-review & editing. **Zhan Tian:** Funding acquisition; writing-review & editing. **Laixiang Sun:** Funding acquisition; writing-review & editing.

ORCID

Shuai Wang  <https://orcid.org/0000-0002-0413-081X>

Zhan Tian  <https://orcid.org/0000-0002-4520-0036>

REFERENCES

- Anthes, R.A. (1982) *Tropical Cyclones-Their Evolution, Structure and Effects*. Boston, MA: The American Meteorological Society.
- Bruneau, N., Wang, S. and Toumi, R. (2020) Long memory impact of ocean mesoscale temperature anomalies on tropical cyclone size. *Geophysical Research Letters*, 47, 1–19. <https://doi.org/10.1029/2019GL086165>.
- Bruyère, C.L., Done, J.M., Jaye, A.B., Holland, G.J., Buckley, B., Henderson, D.J., Lepastrier, M. and Chan, P. (2019) Physically-based landfalling tropical cyclone scenarios in support of risk assessment. *Weather and Climate Extremes*, 26, 1–13.
- Chan, K.T.F. and Chan, J.C.L. (2015) Impacts of vortex intensity and outer winds on tropical cyclone size. *Quarterly Journal of the Royal Meteorological Society*, 141, 525–537.
- Conner, W.C., Kraft, R.H. and Harris, D.L. (1957) Empirical methods for forecasting the maximum storm tide due to hurricanes and other tropical storms. *Monthly Weather Review*, 85, 113–116.
- Daloz, A.S. and Camargo, S.J. (2018) Is the poleward migration of tropical cyclone maximum intensity associated with a poleward migration of tropical cyclone genesis? *Climate Dynamics*, 50, 705–715. <https://www.ncdc.noaa.gov/ibtracs/>.
- De Goede, E.D. (2020) Historical overview of 2D and 3D hydrodynamic modelling of shallow water flows in the Netherlands. *Ocean Dynamics*, 70, 521–539.
- Emanuel, K. (2005) Increasing destructiveness of tropical cyclones over the past 30 years. *Nature*, 436, 686–688.
- Fogarty, E.A., Elsner, J.B., Jagger, T.H., Liu, K.B. and Louie, K.S. (2006) Variations in typhoon landfalls over China. *Advances in Atmospheric Sciences*, 23, 665–677.
- Fudeyasu, H. and Wang, Y. (2011) Balanced contribution to the intensification of a tropical cyclone simulated in TCM4: outer-core spinup process. *Journal of the Atmospheric Sciences*, 68, 430–449. <https://doi.org/10.1175/2010JAS3523.1>.
- Hanson, S., Nicholls, R., Ranger, N., Hallegatte, S., Corfee-Morlot, J., Herweijer, C. and Chateau, J. (2011) A global ranking of port cities with high exposure to climate extremes. *Climatic Change*, 104, 89–111.
- Harris, D.L. (1963) *Characteristics of the Hurricane Storm Surge*. Melbourne, FL: Department of Commerce, Weather Bureau.
- Irish, J.L., Resio, D.T. and Ratcliff, J.J. (2008) The influence of storm size on hurricane surge. *Journal of Physical Oceanography*, 38, 2003–2013.
- Jelesnianski, C.P. (1966) Numerical computations of storm surges without bottom stress. *Monthly Weather Review*, 94, 379–394.
- Jelesnianski, C.P. (1992) *SLOSH: sea, lake, and overland surges from hurricanes*. Tech. Rep. Silver Spring, MD: US Department of Commerce, National Oceanic and Atmospheric Administration, National Weather Service.
- Joyce, B.R., Gonzalez-Lopez, J., Van der Westhuysen, A.J., Yang, D., Pringle, W.J., Westerink, J.J. and Cox, A.T. (2019) U. S. IOOS coastal and ocean modeling testbed: hurricane-induced winds, waves, and surge for deep ocean, reef-fringed Islands in the Caribbean. *Journal of Geophysical Research: Oceans*, 124, 2876–2907.
- Ke, Q., Yin, J., Bricker, J., Savage, N., Buonomo, E., Ye, Q., Visser, P., Dong, G., Wang, S., Tian, Z., Sun, L., Toumi, R. and Jonkman, S. (2021) Typhoon-induced flood hazard increases under climate change: a case study in Shanghai. *Natural Hazards* In print.
- Kernkamp, H.W., Van Dam, A., Stelling, G.S. and De Goede, E.D. (2011) Efficient scheme for the shallow water equations on unstructured grids with application to the continental shelf. *Ocean Dynamics*, 61, 1175–1188.
- Knutson, T.R., Camargo, S.J., Chan, J.C.L., Emanuel, K., Ho, C.-H., Kossin, J., Mohapatra, M., Satoh, M., Sugi, M., Walsh, K. and Wu, L. (2019) Tropical cyclones and climate change assessment: part I: detection and attribution. *Bulletin of the American Meteorological Society*, 100, 1987–2007. <https://doi.org/10.1175/BAMS-D-18-0189.1>.
- Knutson, T.R., Camargo, S.J., Chan, J.C.L., Emanuel, K., Ho, C.-H., Kossin, J., Mohapatra, M., Satoh, M., Sugi, M., Walsh, K. and Wu, L. (2020) Tropical cyclones and climate change assessment: part II: projected response to anthropogenic warming. *Bulletin of the American Meteorological Society*, 101, E303–E322. <https://doi.org/10.1175/BAMS-D-18-0194.1>.
- Knutson, T.R., Sirutis, J.J., Zhao, M., Tuleya, R.E., Bender, M., Vecchi, G.A., Villarini, G. and Chavas, D. (2015) Global projections of intense tropical cyclone activity for the late twenty-first century from dynamical downscaling of CMIP5/RCP4.5 scenarios. *Journal of Climate*, 28, 7203–7224. <https://doi.org/10.1175/JCLI-D-15-0129.1>.
- Knutson, T.R. and Tuleya, R.E. (2004) Impact of CO₂-induced warming on simulated hurricane intensity and precipitation: sensitivity to the choice of climate model and convective parameterization. *Journal of Climate*, 17, 3477–3495.
- Kossin, J.P., Emanuel, K.A. and Camargo, S.J. (2016) Past and projected changes in western north pacific tropical cyclone exposure. *Journal of Climate*, 29, 5725–5739.
- Kossin, J.P., Emanuel, K.A. and Vecchi, G.A. (2014) The poleward migration of the location of tropical cyclone maximum intensity. *Nature*, 509, 349–352. <http://www.nature.com/articles/nature13278>.
- Lavender, S.L. and McBride, J.L. (2020) Global climatology of rainfall rates and lifetime accumulated rainfall in tropical cyclones: influence of cyclone basin, cyclone intensity and cyclone size. *International Journal of Climatology*, 41, 1–19.
- Liu, K.S. and Chan, J.C.L. (2019) Interdecadal variation of frequencies of tropical cyclones, intense typhoons and their ratio over the western North Pacific. *International Journal of Climatology*, 40, 3954–3970. <https://doi.org/10.1002/joc.6438>.
- Martyr-Koller, R.C., Kernkamp, H.W., van Dam, A., van der Wegen, M., Lucas, L.V., Knowles, N., Jaffe, B. and Fregoso, T. A. (2017) Application of an unstructured 3D finite volume numerical model to flows and salinity dynamics in the San Francisco Bay-Delta. *Estuarine, Coastal and Shelf Science*, 192, 86–107. <https://doi.org/10.1016/j.ecss.2017.04.024>.
- Mori, N., Kato, M., Kim, S., Mase, H., Shibutani, Y., Takemi, T., Tsuboki, K. and Yasuda, T. (2014) Local amplification of storm surge by Super Typhoon Haiyan in Leyte Gulf. *Geophysical Research Letters*, 41, 5106–5113. <https://doi.org/10.1002/2014GL060689>.
- Murakami, H., Delworth, T.L., Cooke, W.F., Zhao, M., Xiang, B. and Hsu, P.C. (2020) Detected climatic change in global

- distribution of tropical cyclones. *Proceedings of the National Academy of Sciences of the United States of America*, 117, 10706–10714.
- Park, D.-S.R., Ho, C.-H. and Kim, J.-H. (2014) Growing threat of intense tropical cyclones to East Asia over the period 1977–2010. *Environmental Research Letters*, 9, 014008. <http://stacks.iop.org/1748-9326/9/i=1/a=014008?key=crossref.1768076a048565351c334b902ac24053>.
- Pielke, R.A., Gratz, J., Landsea, C.W., Collins, D., Saunders, M.A. and Musulin, R. (2008) Normalized hurricane damage in the United States: 1900–2005. *Natural Hazards Review*, 9, 29–42.
- Rappaport, E.N. (2014) Fatalities in the United States from atlantic tropical cyclones: new data and interpretation. *Bulletin of the American Meteorological Society*, 95, 341–346.
- Rego, J.L. and Li, C. (2009) On the importance of the forward speed of hurricanes in storm surge forecasting: a numerical study. *Geophysical Research Letters*, 36, 1–5.
- Sharmila, S. and Walsh, K.J. (2018) Recent poleward shift of tropical cyclone formation linked to Hadley cell expansion. *Nature Climate Change*, 8, 730–736. <https://doi.org/10.1038/s41558-018-0227-5>.
- Simpson, R.H. and Saffir, H. (1974) The hurricane disaster potential scale. *Weatherwise*, 27, 169.
- Skamarock, W., Klemp, J., Dudhi, J., Gill, D., Barker, D., Duda, M., Huang, X.-Y., Wang, W. and Powers, J. (2008) A description of the advanced research WRF version 3. *Technical Report*, 113.
- Small, C. and Nicholls, R.J. (2003) A global analysis of human settlement in coastal zones. *Journal of Coastal Research*, 19, 584–599.
- Sun, J., Wang, D., Hu, X., Ling, Z. and Wang, L. (2019) Ongoing poleward migration of tropical cyclone occurrence over the Western North Pacific Ocean. *Geophysical Research Letters*, 46, 9110–9117.
- Sun, Y., Zhong, Z., Li, T., Yi, L., Hu, Y., Wan, H., Chen, H., Liao, Q., Ma, C. and Li, Q. (2017) Impact of ocean warming on tropical cyclone size and its destructiveness. *Scientific Reports*, 7, 8154. <http://www.nature.com/articles/s41598-017-08533-6>.
- Wang, J., Yi, S., Li, M., Wang, L. and Song, C. (2018) Effects of sea level rise, land subsidence, bathymetric change and typhoon tracks on storm flooding in the coastal areas of Shanghai. *Science of the Total Environment*, 621, 228–234.
- Wang, S. and Toumi, R. (2016) On the relationship between hurricane cost and the integrated wind profile. *Environmental Research Letters*, 11, 114005. <http://stacks.iop.org/1748-9326/11/i=11/a=114005?key=crossref.b8c4fd8906504a99c87f1218d5c8042f>.
- Wang, S. and Toumi, R. (2018a) A historical analysis of the mature stage of tropical cyclones. *International Journal of Climatology*, 38, 2490–2505. <https://doi.org/10.1002/joc.5374>.
- Wang, S. and Toumi, R. (2018b) Reduced sensitivity of tropical cyclone intensity and size to sea surface temperature in a radiative-convective equilibrium environment. *Advances in Atmospheric Sciences*, 35, 981–993. <https://doi.org/10.1007/s00376-018-7277-5>.
- Wang, S. and Toumi, R. (2019) Impact of dry midlevel air on the tropical cyclone outer circulation. *Journal of the Atmospheric Sciences*, 76, 1809–1826. <https://doi.org/10.1175/JAS-D-18-0302.1>.
- Weisberg, R.H. and Zheng, L. (2006) Hurricane storm surge simulations for Tampa Bay. *Estuaries and Coasts*, 29, 899–913.
- Wong, B. and Toumi, R. (2016a) Effect of extreme ocean precipitation on sea surface elevation and storm surges. *Quarterly Journal of the Royal Meteorological Society*, 142, 2541–2550.
- Wong, B. and Toumi, R. (2016b) Model study of the asymmetry in tropical cyclone-induced positive and negative surges. *Atmospheric Science Letters*, 17, 334–338.
- Xu, J. and Wang, Y. (2010) Sensitivity of tropical cyclone inner-core size and intensity to the radial distribution of surface entropy flux. *Journal of the Atmospheric Sciences*, 67, 1831–1852.
- Yoshida, K., Sugi, M., Mizuta, R., Murakami, H. and Ishii, M. (2017) Future changes in tropical cyclone activity in high-resolution large-ensemble simulations. *Geophysical Research Letters*, 44, 9910–9917.

SUPPORTING INFORMATION

Additional supporting information may be found online in the Supporting Information section at the end of this article.

How to cite this article: Wang, S., Toumi, R., Ye, Q., Ke, Q., Bricker, J., Tian, Z., & Sun, L. (2021). Is the tropical cyclone surge in Shanghai more sensitive to landfall location or intensity change? *Atmospheric Science Letters*, e1058. <https://doi.org/10.1002/asl.1058>